International Journal of
Research in Chemistry and Environment
Available online at: www.ijrce.org
ISSN 2248-9649

***Research Paper***

# Kinetic, Mechanistic, Equilibrium and Thermodynamic Studies for the Adsorption of Paracetamol on Agricultural based Adsorbents and Nanometal Oxides

**Neha Dhiman, Neeta Sharma**
Dr. SS Bhatnagar University Institute of Chemical Engineering and Technology, Panjab University, 160014 Chandigarh, INDIA

**(Received 04th March 2019, Accepted 28th March 2019)**

***Abstract:*** *There is a global consensus on waste water treatment which is a cause of major concern. A common drug released by pharmaceutical units is paracetamol, it causes hepatitis, nausea and abdominal pain. The present project is an attempt to explore efficient and cost effective adsorbents, the adsorption potential of agricultural based adsorbents and nanometal oxides for paracetamol from aqueous solution has been studied. Analyses of data from experiments at varying parameters affecting adsorption, show that Freundlich and Langmuir isotherm models are obeyed and the process follows pseudo-second-order kinetics in all the cases. A possible mechanism has been proposed. Thermodynamic studies suggest endothermic and spontaneous nature of adsorption. Continuous flow column studies, using sequential bed as well as vertical bed columns, show that breakthrough time and the time for saturation of columns decreases with increase in feed concentration and flow rate. Thomas and Yoon-Nelson models fit well to the experimental data and efficiency of sequential bed column is better than that of vertical column.*

**Keywords:** Paracetamol, Nanometal oxides, Column studies, Adsorption isotherm analyses, Kinetic studies.



## Introduction

Fresh water is a scarce commodity thus the conservation of water resources is extremely important and there is a global consensus on industrial waste water treatment. Pharmaceutical pollutants originate from human excreta as well as pharma industries, as some of the small scale industrial units fail to meet the stringent discharge compliance regulations. The concentration of pharmaceuticals in ground water is in the range 1-100 µg/L and the commonly detected drugs are analgesics and antipyretics[1]. Removal of these pharmaceuticals is of importance because even at low concentrations they present a health hazard. Adsorption has been found to be an effective and highly selective method for the removal of pharmaceutical pollutants at low concentrations[1,2]. Paracetamol (N-acetyl-para-aminophenol) is a very commonly used drug with antipyretic and anti-inflammatory properties[3,4]. Literature reports on batch studies for the removal of paracetamol by adsorption method show the use of activated carbon obtained from agricultural based residues[5,6] and some agricultural by-products[7] as adsorbents. Besides this sugarcane bagasse and sugar pulp[8], pulp mill sludge[9] and Kaolinite clay [10] have also been used. The use of graphene nanoplatelets as adsorbent for paracetamol reveals that these have a better removal efficiency, which is attributed to the small size and large surface area of the adsorbent[4]. There are no reports in literature on the use of continuous flow columns for removal of paracetamol, however, column studies are extremely necessary to ascertain the use of an adsorbent for industrial application. In the present paper, batch as well as continuous flow column studies (using the conventional vertical bed column as well as sequential bed column) have been reported with a view to study and compare the removal efficiency of agricultural based adsorbents namely, wheat *(Triticum Aestivum)* bran and groundnut *Arachis hypogaea)* shell powder with nanometal oxides namely ZnO and CuO

nanoparticles, for paracetamol from aqueous solution. Thermodynamic as well as kinetic studies have also been carried out and an attempt has been made to throw light on the possible mechanism of adsorption.

## Material and Methods

### Preparation of Adsorbent

*Wheat (Triticum Aestivum) bran and groundnut (Arachis Hypogaea) shell powder*

Wheat bran (Bagrry's) and groundnut shells (obtained from local market) were washed properly, dried and ground. The powder was subjected to sieve analysis and particles between 250-420 micron size were retained to be used as adsorbent [11,12].

*ZnO nanoparticles*

Zinc oxide nanoparticles have been prepared by the reported method[13], by the addition of 4.0M NaOH (Merck) solution to 0.2 M $ZnSO_4$ (Merck) solution with stirring at 60ºC. The final pH of the mixture was fixed at 13, precipitation occurs after 2 hr. The obtained precipitates were washed and dried at 60 ºC in an air oven.

*CuO nanoparticles*

CuO nanoparticles have been synthesized by precipitation method[14] by heating 0.02 M copper acetate solution with 1 ml glacial acetic acid in round-bottomed flask equipped with a refluxing device at 100ºC with vigorous stirring. NaOH pellets were added to the boiling solution until pH 6-7 is attained. Black precipitates were obtained. After cooling, the precipitates were centrifuged, washed with distilled water and dried at room temperature.

### Preparation of Adsorbate Solution

Paracetamol injection (INTAS pharmaceuticals Ltd.) 2ml vial containing 150mg of drug has been used to prepare a stock solution of concentration 300mg/L. Dilutions with double distilled water were carried out for obtaining the concentrations required for experiments.

### Estimation of paracetamol

Estimation of the drug was carried out using UV-visible spectrophotometer, (Shimadzu 2450, Japan) with 1 cm optical path length quartz cells using double distilled water as blank[15]. The drug solutions at different pH, in the concentration range 1-12mg/L were analyzed at the respective $\lambda_{max}$. The value of $\lambda_{max}$ at pH 4 is 243nm [15]. Calibration curves were plotted separately for each pH under study.

### Batch Adsorption Studies

Batch experiments to study the effects of initial drug concentration (10-100mg/L), pH in the range 3-11, (precipitation occurs below pH 3), and contact time have been studied. A known weight of adsorbent (100mg) was placed in contact with 10 ml of adsorbate solution with constant stirring for regular time intervals (until equilibrium is attained)[16]. The pH of the solution was adjusted using 0.1M HCl/NaOH as required. After adsorption the concentration of the drug was determined spectrophotometrically[14,15]. All experiments have been carried out in triplicate to ascertain reproducibility.

### Column Adsorption Studies

Continuous flow column studies have also been carried out using vertical as well as sequential bed adsorption columns at varying initial drug concentration (80-100mg/L) and flow rate (5ml/min. to 10ml/min.) at the pH of maximum adsorption for each adsorbent.

### Experimental Setup

*Vertical column*

A vertical column of 1.5cm diameter and 20cm height was set up. The down flow mode was used and the flow through the column maintained using a rotameter[13]. The adsorbent is packed up to a depth of 4cm (7.2gm wheat bran, 4gm groundnut shell powder, 5.2gm ZnO nanoparticles and 4.2gm CuO nanoparticles) in the column (obtained from Bed Depth Service Time (BDST) model). After adsorption, samples are withdrawn at regular intervals of time and analysed for drug concentration.

*Sequential bed column*

Sequential bed column was prepared by connecting 4 glass tubes of 1.5cm diameter in such a way that it can contain the adsorbent at each step, without using any support, for free flow of adsorbate solution under gravity[13]. The first tube, filled with solid adsorbent, received the influent which flowed through the second tube and so on. The amount of adsorbent taken in each tube is equal to $1/4^{th}$ part of total weight of adsorbent taken in vertical column. The flow rate is controlled in such a way that contact time of adsorbate and adsorbent is in the range of 3-4 hrs. Samples have been collected from the end of the column, at regular intervals of time, to determine the drug concentration.

### Breakthrough Curves

To evaluate the performance of continuous flow adsorption column, a study of breakthrough curves is desirable. The breakthrough curve is expressed as a plot of $C_t/C_o$ against time of contact (t), where $C_t/C_o$ is ratio of effluent concentration ($C_t$) to the adsorbate inlet concentration ($C_o$). The breakthrough point occur when effluent concentration, $C_t = 0.5C_o$ and column is considered to be saturated when $C_t = 0.9C_o$ [13].

*Effect of initial drug concentration and flow rate*

Three different feed concentrations i.e, 80mg/L, 90mg/L and 100mg/L at the influent flow rate of 5ml/min., 7.5ml/min., 10ml/min. for each

concentration have been studied using both vertical bed and sequential bed adsorption columns

## Results and Discussion

### Characterization of agricultural based adsorbents

*Proximate analysis*

Proximate analyses to determine moisture, ash and volatile matter were carried out by heating 5gm sample in each case, upto 700°C. The moisture content was found to be 7.8% for wheat bran and 9.7% for groundnut shell powder. The ash content was found to be 3.90% for wheat bran and 7% for groundnut shell powder at 700°C[13,17].

*Fourier Transform Infrared (FTIR) Spectral Studies*

*(a) Wheat (Triticum aestivum) Bran*

FTIR spectrum of wheat bran shows band at 3433.24cm$^{-1}$ attributed to the surface hydroxyl groups (O-H) and chemisorbed water. Peak at 2932.04cm$^{-1}$ and 1649.0cm$^{-1}$ corresponding to symmetric or asymmetric stretching vibrations of C-H group, and stretching vibrations of carbonyl group (C=O) respectively. Peaks at 1535.97 to 1337.55cm$^{-1}$ have been attributed to bending vibrations of carboxylate ion. The peak at 1151.80cm$^{-1}$ may be assigned to stretching mode of proteins (-CN) and that at 1029.0 cm$^{-1}$ due to C-O bond of cellulose[11].

*(b) Groundnut (Arachis hypogaea) Shell Powder*

Groundnut shell powder shows band at 3405.71cm$^{-1}$ assigned to the O-H stretching of alcohols and phenols. Peak at 2928.66cm$^{-1}$ indicative of symmetric or asymmetric stretching vibrations of C-H group,at 1731.47cm$^{-1}$ corresponding to ester and acetyl group of hemicelluloses. The peaks at 1638.86cm$^{-1}$, 1512.69 to 1331.64cm$^{-1}$ confirm the presence of lignin and peaks at 1260.83cm$^{-1}$ and 1151.80cm$^{-1}$ are attributed to hydrogen bonding[13].

### Characterisation of nanoparticles

*X-ray diffraction (XRD)*

The XRD pattern of ZnO nanoparticles shows peaks at scattering angle (2$\theta$) of 31.7288, 34.3877, 36.2432, 47.5063, 56.5137 and 62.8756, which correspond to the reflection from (100), (002), (101), (102), (110) and (103) planes, respectively, it can be inferred that the nanoparticles are pure zinc oxide with a hexagonal structure[13] ( Figure 1.a).

The XRD pattern of CuO nanoparticles (Figure 1.b) shows peaks at scattering angle(2θ) of 32.5265, 35.5022, 38.6928, 53.5068, 58.1202, 61.0685, 68.0489 corresponding to the reflection from (111), (111), (202), (020), (202), (113), (311) planes[14] respectively. The XRD pattern indicates a single-phase CuO with a monoclinic structure. The average diameter of synthesized ZnO and CuO nanoparticles calculated using Debye-Scherrer's formula,

$$D = 0.89\,\lambda/b\,\cos\theta \qquad (1)$$

Where 0.89 is the Scherrer's constant, $\lambda$ is the plane located at 36.24° for ZnO nanoparticles and 38.69$^0$ for CuO nanoparticles, was found to be 68.61nm for ZnO [13] and 19.96nm for CuO nanoparticles[14].

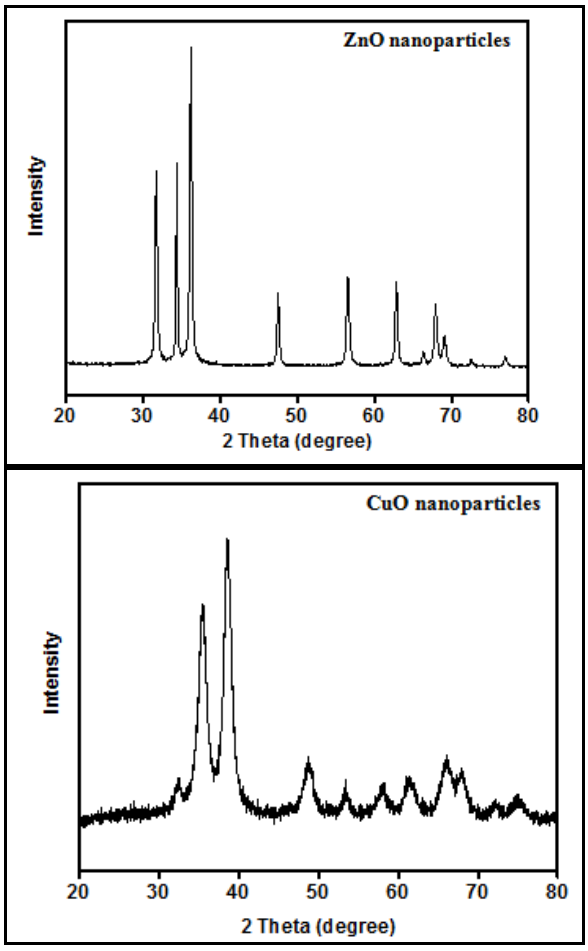


**Figure 1: XRD pattern of (a) ZnO nanoparticles and (b) CuO nanoparticles**

*Transmission electron microscopy* (*TEM )*

The average particle size of ZnO was estimated to be 100nm[13] and that for CuO was found to be 20nm, further the TEM image of CuO nanoparticles indicates that the particles are needle shaped[14]

*Fourier Transform Infrared (FTIR) Spectral Studies*

*(a) ZnO Nanoparticles*

FTIR spectrum of ZnO nanoparticles shows bands at 3499.70 cm$^{-1}$, 3394.82cm$^{-1}$ attributed to surface hydroxyl groups (O-H). Bands between 1510.50 to 1391.06 cm$^{-1}$ may be assigned to bending mode of water molecules and a peak at 505.67 cm$^{-1}$ is the characteristic peak of Zn-O bond[13].

*(b) CuO Nanoparticles*

A band at 3442.16cm$^{-1}$ is indicative of surface hydroxyl groups (O-H) and the peaks observed between 1565.91 to 1343.17cm$^{-1}$ may be attributed to bending of water molecules. A peak at 528.35cm$^{-1}$ is due to the Cu-O bond[18].

**Effect of pH and Point zero charge ($pH_{pzc}$)**

The structural forms of paracetamol at different pH values are:

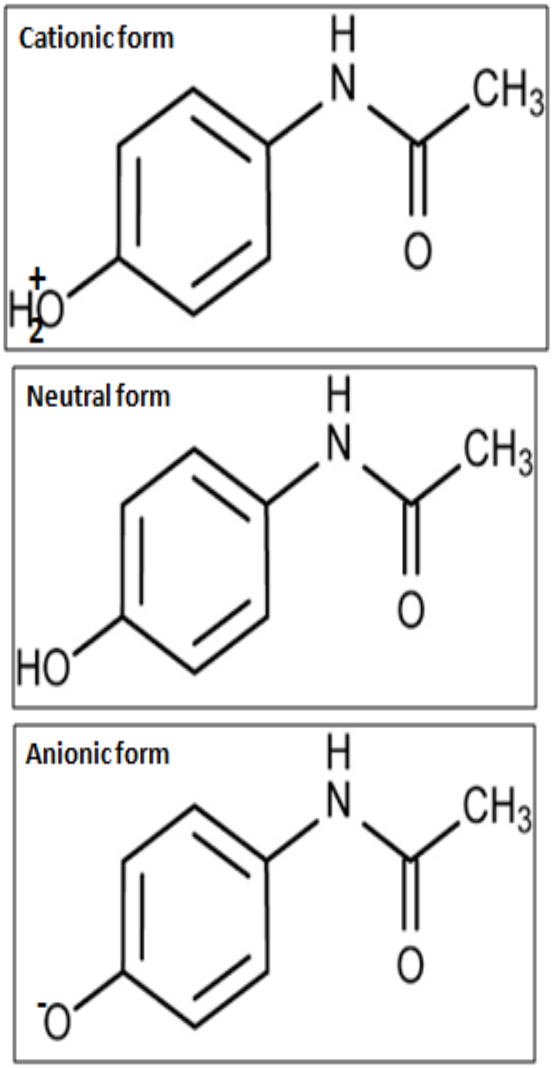


paracetamol exists in protonated form, upto pH 7, in between pH 7 to 9.5 the proton of the phenol group is removed and paracetamol becomes completely neutral and its solubility in water also decreases, above pH 9.5 paracetamol has net negative charge.

Adsorption of paracetamol has been found to increase with increase in pH in the range 3-11 and maximum adsorption is obtained at pH 7 for wheat bran and groundnut shell powder and at pH 8 for ZnO and CuO nanoparticles (Figure 2).

The surface charge of the adsorbent (point zero charge) which is dependent upon the presence of $H^+$ and $OH^-$ ions on the surface of the adsorbent also plays an important role. The $pH_{pzc}$ values have been determined to be 6.2 for wheat bran and 6.4 for groundnut shell powder which are in concurrence with the reported values[11,12], the reported pKa value of paracetamol is 9.5[1]. Above pH 6, the surface of both the adsorbents is negatively charged, while paracetamol carries a net positive charge, which attributes to the maximum adsorption of drug at pH 8 for wheat bran and pH 9 groundnut shell powder. Similarly for ZnO the value of $pH_{pzc}$ have been found to be 8.75 [13] and for CuO nanoparticles it is 7.35 [19], which shows that both the adsorbents are negatively charged at pH 9, hence adsorption is favorable.

**Effect of Initial Concentration and Contact Time**

Batch experiments carried out for the concentration range 10-100mg/L at varying pH (3-11) for varying time of contact, till the attainment of equilibrium, at 25$^0$C show that the amount adsorbed increases with increase in concentration and contact time. Equilibrium is attained within 165min. for wheat bran and ZnO nanoparticles and 180min. for groundnut shell powder and CuO nanoparticles. In the initial stages the adsorption is rapid which can be attributed to the availability of larger number of surface sites in the beginning. As the available sites get occupied adsorption rate decreases[13,16].

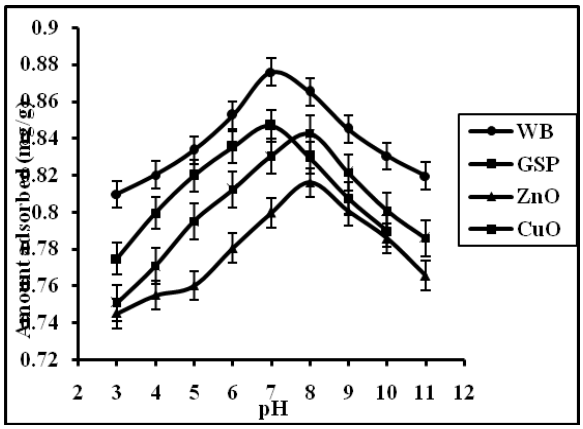


**Figure 2: Effect of pH on amount of paracetamol adsorbed at drug concentration 100mg/L using wheat bran (WB), groundnut shell powder (GSP), ZnO and CuO nanoparticles**

**Adsorption Isotherm Modelling**

*Freundlich isotherm*

The linearised form of the Freundlich equation is:

$$\log q_e = \log K_f + {}^1/_n \log C_e \qquad (2)$$

where $C_e$ is the equilibrium concentration (mgL$^{-1}$) and $q_e$ is the amount adsorbed (mgg$^{-1}$). The values of n and $K_f$ ,as determined from slope and intercept of the linear

plot of log $q_e$ vs. log $C_e$, are presented in Table 1. The value of 1<n<10 suggests effective and monolayer adsorption for each adsorbent[20] [20].

*Langmuir adsorption isotherm*

Langmuir equation is given by:

$$C_e/q_e = 1/K_L + a_L/K_L \; C_e \quad (3)$$

where $C_e$ is the solute phase concentration(mg/L), $q_e$ is the amount of solute adsorbed per unit weight of adsorbent(mg/g), $K_L$ related to affinity of the binding sites ($Lmg^{-1}$) and $a_L$ the Langmuir isotherm constant determined from a straight line plot of $C_e/q_e$ against $C_e$ (Table1). The adsorption data for all the adsorbents fits well to the Langmuir isotherm model[20] [20].

Feasibility of the isotherm can be expressed in terms of separation factor or equilibrium parameter $R_L$,

$$R_L = 1/(1 + a_L \; C_e) \quad (4)$$

The values of $R_L$ have been found to be 0.31, 0.23, 0.23 and 0.31 for wheat bran, groundnut shell powder, ZnO and CuO nanoparticles respectively indicates favorable adsorption in each case[20].

*Temkin isotherm*

Temkin equation is given as,

$$q_e = B_T \; ln \; A_T + B_T \; ln \; C_e \quad (5)$$

Where, $q_e$ is the amount of solute adsorbed per unit weight of adsorbent(mg/g), $B_T$ is constant related to heat of adsorption ($Jmol^{-1}$), $A_T$ is the equilibrium binding constant ($Lg^{-1}$), T is absolute temperature (K) and R is universal gas constant, 8.314 J $mol^{-1}$ $K^{-1}$ [1,5]. The values of the isotherm constants are given in (Table 1). A straight line plot of $q_e$ vs. ln $C_e$ indicates that Temkin isotherm is followed.

**Error Analysis for Isotherm Studies**

To evaluate the fit of isotherm models, the error values can be calculated using five different error functions of non-linear regression as follow [21]:

*Sum of squared errors (SSE):*

$$SSE = \sum_{i=1}^{n} (q_{e,cal} - q_{e,exp})^2 \quad (6)$$

*Sum of absolute errors (SAE):*

$$SAE = \sum_{i=1}^{n} | q_{e,cal} - q_{e,exp} |_i \quad (7)$$

*Average relative error (ARE):*

$$ARE = \frac{100}{n} \sum_{i=1}^{n} \left| \frac{q_{e,cal} - q_{e,exp}}{q_{e,exp}} \right| \quad (8)$$

*Hybrid fractional error function (HYBRID):*

$$HYBRID = \sum_{i=1}^{n} \left[ \frac{(q_{e,exp} - q_{e,cal})^2}{q_{e,exp}} \right]_i \quad (9)$$

*Marquardt's percent standard deviation (MPDS):*

$$MPSD = \sum_{i=1}^{n} \left[ \frac{q_{e,exp} - q_{e,cal}}{q_{e,exp}} \right]^2 \quad (10)$$

The results from the error function values suggest that Freundlich and Langmuir isotherm models show a good fit for all the adsorbents studied except for groundnut shell powder where Freundlich and Temkin isotherm models are a better fit[21].

**Kinetic Studies**

*Pseudo first order equation*

$$log \; (q_e - q) = log \; q_e - k_{ad} \; X \; t/2.303 \quad (11)$$

where $q_e$ and q (mg $g^{-1}$) are the amounts of drug adsorbed at equilibrium and at any time t, t (min) is the time of contact and $k_{ad}$ is the adsorption rate constant ($min^{-1}$) [1]. The values of rate constant $k_{ad}$ ($min^{-1}$) and $q_e$ ($mgg^{-1}$) have been calculated using slope and intercept of plot log($q_e$ − q) vs. t and are given in Table 1.

*Pseudo second order equation*

Pseudo second order equation is given as,

$$t/q = 1/K_2 \; X \; 1/q_e^2 + t/q_e \quad (12)$$

where $K_2$ is equilibrium rate constant of pseudo second order adsorption ($gmg^{-1}$ $min^{-1}$), $q_e$ and q (mg $g^{-1}$) is the amount of paracetamol adsorbed at equilibrium and at any time and t (min) is the time of contact[5]. A straight line plot of t/q vs. t suggests applicability of the model [1] the values of rate constants $K_2$ and $q_e$ are given in Table 1.

*Intra-Particle Diffusion Study*

The possibility of intra-particle diffusion has been studied by Morris Weber model,

$$q = K_p \; x \; t^{1/2} \quad (13)$$

where q is the amount of drug adsorbed in mg per g of adsorbent at different time intervals ($mgg^{-1}$), $K_p$ is the intraparticle diffusion constant ($mgg^{-1}$ $min^{-1}$) and t is contact time (min.). $K_p$ as calculated from the slope of the linear plot of q vs $t^{1/2}$ and has been found to be 3.568, 3.634, 3.229 and 2.972 $mgg^{-1}$ $min^{-1}$ for wheat bran, groundnut shell powder, ZnO and CuO nanoparticles respectively. Straight line plots which do not pass through origin have been obtained in each case, which suggests that intraparticle diffusion occurs but is not the rate determining step [1,5].

**Effect of temperature**

Adsorption data for paracetamol on all the adsorbents studied has been obtained at varying temperatures in the range 25° - 45° C, drug concentration of 100mg/L , for adsorbent dose 100mg and at the pH of maximum adsorption and equilibrium contact time for each adsorbent. It has been found that the amount of paracetamol adsorbed increases with increase in temperature from 298K to 318K ,which may be due to increase in number of sorption sites generated because of breaking of some internal bonds near the active surface sites of adsorbent in each case[1].

*Determination of Thermodynamic Parameters*

Thermodynamic parameters such as change in free energy $\Delta G^0$ (KJ/mol), enthalpy ($\Delta H^0$) (KJ/mol) and entropy ($\Delta S^0$) (J/K/mol) have been calculated using the equations:

$$\Delta G^{o} = -RT \ln K_c \quad (14)$$

$$\log K_c = {}^{\Delta S^{o}}/_{(2.303R)} - {}^{\Delta H^{o}}/_{(2.303RT)} \quad (15)$$

where $K_0 = C_{solid}/C_{liquid}$ is the equilibrium constant, $C_{soild}$ is the solid phase concentration of adsorbate at equilibrium (mg/L), $C_{liquid}$ is the liquid phase concentration at equilibrium (mg/L), T is the temperature in degree Kelvin and R is gas constant[1].

The values for change in enthalpy ($\Delta H^0$), entropy ($\Delta S^0$) and Gibbs free energy have been calculated from Van't Hoff plot and are shown in Table 1. The negative values of $\Delta G^0$ for all the adsorbents indicate feasibility and spontaneous nature of adsorption. The positive values of $\Delta H^0$ and $\Delta S^0$ suggests the endothermic nature of adsorption and increase in randomness at solid - solution interface[1].

**Table 1: Isotherm constants, kinetic constants and thermodynamic parameters for adsorption of paracetamol on wheat bran, groundnut shell powder, ZnO nanoparticles and CuO nanoparticles**

| | Wheat bran | Groundnut shell powder | ZnO nanoparticles | CuO nanoparticles |
|---|---|---|---|---|
| **Freundlich** | | | | |
| **n** | 1.63 | 1.65 | 2.12 | 1.74 |
| **$K_f$ (mg/g)** | 1.89 | 1.94 | 1.88 | 1.70 |
| **$R^2$** | 0.990 | 0.974 | 0.988 | 0.995 |
| **Langmuir** | | | | |
| **$a_L$ (mg/g)** | 0.177 | 0.20 | 0.176 | 0.15 |
| **$K_L$ (L/mg)** | 2.12 | 2.32 | 1.69 | 1.72 |
| **$R^2$** | 0.950 | 0.985 | 0.904 | 0.955 |
| **Temkin** | | | | |
| **$A_T$ (L/g)** | 2.64 | 2.69 | 4.13 | 2.24 |
| **$B_T$ (J/mol)** | 2.217 | 2.201 | 1.561 | 2.040 |
| **$b_T$** | $11.17x10^2$ | $11.25x10^2$ | $15.86x10^2$ | $12.13x10^2$ |
| **$R^2$** | 0.926 | 0.955 | 0.857 | 0.900 |
| **Pseudo-first order** | | | | |
| **$K_{ad}$ ($min^{-1}$)** | 0.020 | 0.018 | 0.016 | 0.017 |
| **$q_e$ (mg/g)** | 6.15 | 6.29 | 4.96 | 5.21 |
| **$R^2$** | 0.870 | 0.927 | 0.908 | 0.868 |
| **Pseudo-second order** | | | | |
| **$q_e$ (mg/g)** | 9.80 | 9.65 | 8.99 | 9.12 |
| **$K_2$ ($gmg^{-1}$ $min^{-1}$)** | $4.47 \times 10^{-3}$ | $3.65 \times 10^{-3}$ | $4.76 \times 10^{-3}$ | $5.21 \times 10^{-3}$ |
| **$R^2$** | 0.979 | 0.979 | 0.972 | 0.978 |
| **Thermodynamic parameters** | | | | |
| **$\Delta G^0$ (KJ/mol)** | $-48.11 \times 10^2$ | $-42.11 \times 10^2$ | $-36.66 \times 10^2$ | $-41.30 \times 10^2$ |
| **$\Delta H^0$(KJ/mol)** | 0.895 | 0.364 | 0.587 | 0.460 |
| **$\Delta S^0$(KJ/mol)** | 3.218 | 1.420 | 2.134 | 1.738 |

**Estimation of parameters for column design**

To determine the relationship between bed depth (Z) and service time (t), the bed depth service time (BDST) model has been used[13]. The BDST equation can be represented as:

$$t = (N_o Z/C_o Q) - (1/K_a C_o) \ln(C_o/C_t - 1) \quad (17)$$

where $C_o$ is the feed concentration (mg $L^{-1}$), $C_t$ is the breakthrough drug concentration (mg $L^{-1}$), Q is the linear flow rate of adsorbate (cm $min^{-1}$), $N_o$ the sorption capacity of bed (mg $L^{-1}$). From the slope and intercept of a linear plot of bed depth (Z) against service time t, the values of design parameters; adsorption capacity of bed ($N_o$) and kinetic constant ($K_a$) can be determined, where slope = $N_o/C_o Q$ and intercept = $(1/K_a C_o) \ln(C_o/C_t - 1)$.

**Column Adsorption Study**

*Effect of Influent drug Concentration*

The drug concentration has been varied in the range 80 to 100mg/L at flow rate of 5ml/min. for vertical as well as sequential adsorption column. It has been observed that the removal efficiency decreases with increase in concentration of paracetamol, for each adsorbent. This can be explained on the basis that as the concentration

of paracetamol increases, the number of drug molecules which are in contact with the adsorbent during the same interval of time also increases. While on the other hand the number of sites available for adsorption is constant and become saturated rapidly hence removal efficiency decreases[20].

*Effect of Flow Rate*

Flow rates have been varied from 5ml/min. to 7.5ml/min. to 10ml/min. for an influent concentration of 80mg/L both for vertical as well as sequential bed columns. It has been found that with increase in flow rate, the time required to reach the exhaustion decreases due to lesser residence time of solution in bed which leads to lesser mass transfer due to lesser adsorption [1,20].

*Analyses of Breakthrough Curves*

The breakthrough curves have been obtained by plotting the ratio of effluent concentration ($C_t$) to the adsorbate inlet concentration ($C_o$) i.e. $C_t/C_o$ against time[1]. Breakthrough time corresponding to $C_t/C_o = 0.5$ and the exhaustion time corresponding to $C_t/C_o = 0.90$ was obtained at drug concentration 80mg/L for all the adsorbents using vertical bed as well as sequential bed column.

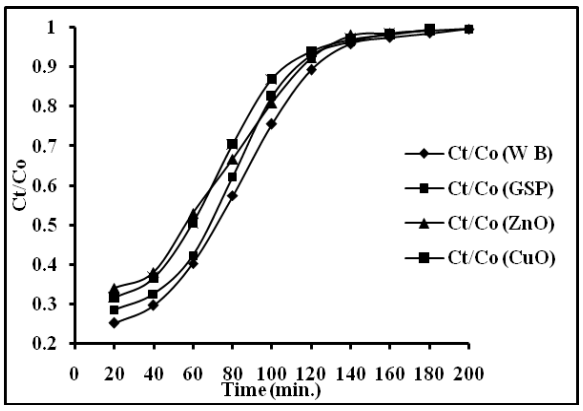


**Figure 3: Breakthrough curves for adsorption of paracetamol in vertical column using wheat bran (WB), groundnut shell powder (GSP), ZnO nanoparticles and CuO nanoparticles at flow rate 5ml/min. and drug concentration 80mg/L**

Breakthrough point occurred after 85min. for wheat bran, 75min. for groundnut shell powder and 70min. for both ZnO nanoparticles and CuO nanoparticles in sequential bed adsorption column. For vertical bed column breakthrough occurred at 70min for both wheat bran and groundnut shell powder, 55min. for ZnO nanoparticles and 60min. for CuO nanoparticles. While the exhaustion time for the vertical bed adsorption column was found to be 125min. for wheat bran and 115min. for groundnut shell powder, ZnO and CuO and for sequential adsorption column it is 135min. for wheat bran, groundnut shell powder and ZnO and 120min. for CuO (Figure 3 and Figure 4).

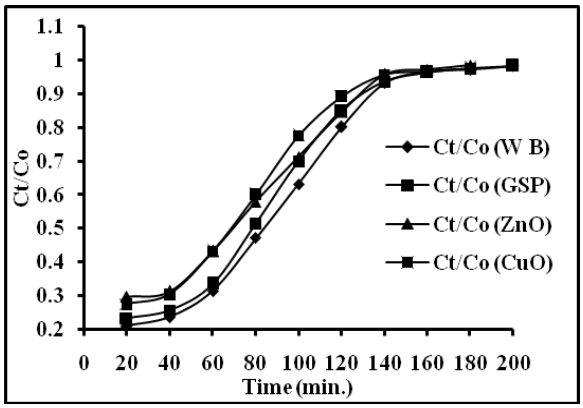


**Figure 4: Breakthrough curves for adsorption of paracetamol in sequential bed column using wheat bran (WB), groundnut shell powder (GSP), ZnO nanoparticles and CuO nanoparticles at flow rate 5ml/min. and drug concentration 80mg/L**

As the drug concentration increases, the curve becomes steeper, the breakthrough time and amount adsorbed decreases also at a higher influent concentration the column is saturated earlier on because the binding sites became saturated more quickly. In contrast, lower influent concentration and longer contact time, resulted in a extended breakthrough curve and mass transfer zone, indicating that maximum adsorbate solution can be treated[1].

**Modeling of Breakthrough Curves**

The data have been subjected to analyses using Thomas model and Yoon–Nelson model.

*Thomas model*

The Thomas model is one of the most general and widely used methods in column performance theory. The linear form of the model is given as:

$$ln\left[{}^{C_o}/_{C_t} - 1\right] = {}^{K_{TH}\, q_o\, M}/_{Q} - K_{TH}\, C_o\, t \qquad (18)$$

Where $K_{TH}$ is Thomas rate constant (L $min^{-1}mg^{-1}$); $q_o$ the maximum solid - phase concentration of the solute (mg $g^{-1}$), M is the mass of adsorbent (g); Q the flow rate (L $min^{-1}$). The kinetic coefficient $K_{TH}$ and the adsorption capacity of the bed $q_o$ can be determined from plot of $[\ln(C_o/C_t)-1]$ against time at a given flow rate[22,23]. The values of $K_{TH}$ (L $min^{-1}mg^{-1}$) and $q_o$ (mg/g) for vertical and sequential bed column are given in Table 2. The value of adsorption capacity $q_o$ (mg/g) has been found to be greater for sequential bed as compared to vertical bed column which can be explained on the basis that the adsorbate comes in contact with a fresh adsorbent on moving from one bed to the other.

Results suggest that Thomas model fits well to the experimental data at the examined flow rate for each adsorbent in both type of columns. However, increase in initial drug concentration shows a significant decrease in the values of $K_{TH}$ and $q_o$ and with increase in flow rate the values of $K_{TH}$ and $q_o$ increase. This may be due to the fact that the concentration difference of adsorbate on the adsorbent and in solution is the only driving force for adsorption[22,24].

*The Yoon–Nelson model*

This model is based on the fact that the rate of decrease in the probability of adsorption for each adsorbate molecule is proportional to the probability of adsorbate adsorption and the probability of adsorbate breakthrough on the adsorbent[24] [24]. The linearised model is expressed as:

$$\ln {}^{C_t}/_{C_o} - C_t = K_{YN}t - \tau K_{YN} \quad (19)$$

where $K_{YN}$ is the rate constant (l $mg^{-1}$), $\tau$ the time required for 50% adsorbate breakthrough (min). The kinetic coefficient $K_{YN}$ and $\tau$ can be determined from a plot of $[\ln(C_t/C_o)-C_t]$ against time t at a given adsorption conditions (Table 2). A straight line plot with slope $K_{YN}$ and intercept $\tau$ suggests applicability of the model[24,25], it has been observed that with increase in initial drug concentration and flow rate, the value of $K_{YN}$ increases and time taken for 50% breakthrough decreases for each adsorbent for both sequential bed and vertical columns[25].

**Table 2: Kinetic coefficients for modeling of breakthrough curves for adsorption of paracetamol on wheat bran, groundnut shell powder, ZnO and CuO nanoparticles**

| | Wheat bran | | Groundnut shell powder | | ZnO nanoparticles | | CuO nanoparticles | |
|---|---|---|---|---|---|---|---|---|
| **Thomas model** | | | | | | | | |
| | **Vert.** | **Seq.** | **Vert.** | **Seq.** | **Vert.** | **Seq.** | **Vert.** | **Seq.** |
| **$K_{TH}$** | $2.53\times10^{-4}$ | $2.28\times10^{-4}$ | $2.61\times10^{-4}$ | $2.23\times10^{-4}$ | $2.56\times10^{-4}$ | $2.26\times10^{-4}$ | $2.63\times10^{-4}$ | $2.27\times10^{-4}$ |
| **$q_o$ (mg/g)** | 6.04 | 7.21 | 9.87 | 12.1 | 6.70 | 8.14 | 8.22 | 9.86 |
| **$R^2$** | 0.966 | 0.971 | 0.975 | 0.9805 | 0.956 | 0.944 | 0.968 | 0.979 |
| **Yoon- Nelson model** | | | | | | | | |
| **$K_{YN}$** | 0.0203 | 0.0183 | 0.0209 | 0.0179 | 0.0205 | 0.0181 | 0.0211 | 0.0182 |
| **$\tau$ ( min)** | 108.46 | 129.35 | 98.72 | 121.12 | 87.10 | 106.08 | 85.95 | 103.37 |
| **$R^2$** | 0.966 | 0.971 | 0.975 | 0.9805 | 0.955 | 0.943 | 0.9683 | 0.979 |

**Fourier Transform infrared FTIR Spectral Studies**

*FTIR of Paracetamol*

FTIR spectrum of paracetamol shows peak at 3319.9 $cm^{-1}$ attributed to the surface hydroxyl group (O-H) stretching. Peak at 1661.2 cm-1 corresponds to C=O amide stretching. The band present at 1554.0 $cm^{-1}$ represents amide II group. The peak at 1253.5 $cm^{-1}$ is attributed to C-N-H group and at 834.9 $cm^{-1}$ may be attributed to para-disubstituted aromatic ring.

*FTIR of the adsorbents after adsorption of paracetamol*

There is no significant change in the infrared spectra of the adsorbents except for the occurrence of a peak around 837 $cm^{-1}$ which is characteristic of paracetamol, due to the presence of para-disubstituted aromatic ring, and hence confirms the presence of paracetamol on the adsorbent surface in each case.

**Mechanism of Adsorption of Paracetamol on each Adsorbent**

The adsorption mechanism for the removal of paracetamol using different adsorbents at varying pH can be explained on the basis of point zero charge of adsorbents and pKa value of paracetamol. The reported pKa value of paracetamol is 9.5 [26].

The values of point zero charge for wheat bran and groundnut shell powder have been found to be 6.2 and 6.4 respectively. At pH above point zero charge, both adsorbents have overall negative charge and since paracetamol exists in protonated form upto pH 7, therefore due to electrostatic attraction between positively charged paracetamol and negatively charged surface of adsorbents, maximum removal occurs at pH 7 for wheat bran and groundnut shell powder. In case of ZnO and CuO nanoparticles the value of point zero charge is 8.7 and 7.5 respectively and at pH above the value of point zero charge, both adsorbents have net positive charge on the surface. Above pH 7 paracetamol is neutral, which indicates that electrostatic interaction does not play any role for the adsorption of paracetamol on ZnO and CuO nanoparticles. Maximum removal was obtained at pH 8 for ZnO and CuO nanoparticles so there may exist some other adsorption mechanism based on hydrogen bonding or hydrophobic interactions[26]. Above pKa value i.e 9.5 paracetamol has net negative charge and the surface of each adsorbent also becomes negatively

charged, which leads to greater repulsion between adsorbate and adsorbent at higher pH [26].

*Maximum adsorption observed at pH 7 for wheat bran and groundnut shell powder:*

$[(PARA)OH_2^+]$ + Negative surface of adsorbent ——— Electrostatic attraction
(Cationic $PARA^+$) ($pH_{pzc}$ of wheat bran 6.2)
($pH_{pzc}$ of groundnut shell powder 6.4)

*In between pH 7-9.5*

[(PARA)OH] ——— Neutral molecule

*Maximum adsorption observed at pH 8 for ZnO and CuO nanoparticles:*

[(PARA)OH] + Surface of adsorbent ——— Hydrophobic interaction
(Neutral molecule) ($pH_{pzc}$ of ZnO 8.7 and CuO 7.5)

*At highly basic conditions:*

$[(PARA)O^-]$ —($OH^-$ ions)— Adsorption decreases
(Anionic $PARA^-$) Compete with anionic $PARA^-$

**Conclusion**

From the study it can be inferred that taking into consideration the cost factor as well as the removal efficiency, agricultural based adsorbents can be termed to be better adsorbents as compared to nano metal oxides as the maximum adsorption capacity does not vary to a large degree. Though nanometal oxides have high selectivity especially for pollutants at low concentration and should be recyclable but the cost of procurement is greater. Efficiency of sequential bed adsorption column has been found to be greater than that of vertical column and considering the experimental setup for sequential column, which is simple and cost effective, it can be considered to have a greater applicability especially in small scale industries.

**Acknowledgment**

One of the authors Neha Dhiman is grateful to Department of Science and Technology, New Delhi, India for grant of Junior Research Fellowship (concurrence Dy. No. C/3260/IFD/2017-18) under INSPIRE Scheme.

**References**

1. Yusoff N. A., Ngadi N., Alias H., Jusoh M., Chemically treated chicken bone waste as an efficient adsorbent for removal of acetaminophen, *Chem. Eng. Trans.* **56,** 925-930 **(2017)**.

2. Ribeiro A. V. F. N., Belisario M., Galazzi R.M., Balthazar D.C., Pereira M. de G., Ribeiro J. N., Evaluation of two bioadsorbents for removing paracetamol from aqueous media, *Electron. J. Biotechnol.* **14,** 1-7 **(2011)**.

3. Syed Draman S. F., Batraazman I. A., Mohd N., Removal of paracetamol from aqueous solution by dried cellulose and activated carbon, *ARPN J. Eng. Appl. Sci.* **10,** 9544 – 48 **(2015)**.

4. Al-Khateeb, Lateefa A., Almotiry S., Salam M.A., Adsorption of pharmaceutical pollutants onto graphene nanoplatelets, *Chem. Eng. J.* **248,** 191-99 **(2014)**.

5. Nche N.A.G., Bopda A., Tchuifon D.R.T., Ngakou C.S., Kuete I.H.T., Gabche A.S., Removal of Paracetamol from Aqueous Solution by Adsorption onto Activated Carbon Prepared from Rice Husk, *J. Chem. Pharm. Res.* **9,** 56-68 **(2017)**.

6. Mukoko T., Mupa M., Guyo U., Dziike F., Preparation of Rice Hull Activated Carbon for the Removal of Selected Pharmaceutical Waste Compounds in Hospital Effluent, *J. Environ. Anal. Toxicol***. 7,** 1-9 **(2015)**

7. Mansour F., Al-Hindi M., Yahfoufi R., Ayoub G.M., Ahmad M.N., The use of activated carbon for the removal of pharmaceuticals from aqueous solutions: a review, *Rev. Environ. Sci. Biotechnol.* **17,** 109-145 **(2018)**

8. Khan M.A., Saeed K., Abdullah W. Ahmad, Mabood F., Rehman M., In Vitro Adsorption of Drugs Using Modified Sugarcane Bagasse, *J. Sci. Ind. Res.* **71,** 161-167 **(2012)**

9. Coimbra R.N., Calisto V., Ferreira C.I.A., Esteves V.I., Otero M., Removal of

Pharmaceuticals from Municipal Wastewater by Adsorption onto Pyrolyzed Pulp Mill Sludge, *Arab. J. Chem*. 1-10 **(2015);** (DOI): 10.1016/j.arabjc.2015.12.

10. Chigbundu E.C., Odigie O.I., Adsorption of Acetaminophen from Aqueous Solutions onto Hexadecyltrimethylammonium Modified Kaolinite, *Nat. Sci.* **12,** 147 **(2014)**

11. Alzaydien A.S., Adsorption Behavior of Methyl Orange onto Wheat Bran : Role of Surface and pH, *Orient. J. Chem*. **31,** 643-651 **(2015)**

12. Adebayo O.L., Ogunmodede O.T., Ojo O.I., Assesment of Ground Nut Husk as a Sorbent in the Decolourization of Congo Red Contaminated Aqueous Medium, *World J. Chem.* **10,** 11-17 **(2015)**

13. Dhiman N., Sharma N., Removal of ciprofloxacin hydrochloride from aqueous solution using vertical bed and sequential bed columns, *J. Environ. Chem. Eng.* **6,** 4391-4398 **(2018)**

14. Sharma N., Dhiman N., Kinetic and Thermodynamic Studies for Ciprofloxacin Hydrochloride Adsorption from Aqueous Solution on CuO Nanoparticles, *Int. J. Chem. Tech Res.* **10 ,** 098-106 **(2017)**

15. Behera S., Ghanty S., Ahmad F., Santra S., Banerjee S., UV-Visible Spectrophotometric Method Development and Validation of Assay of Paracetamol Tablet Formulation, *J.Anal. Bioanal.Tech*. **3,**1-6 **(2012)**

16. Sharma N., Kaur K., Kaur S., Kinetic and equilibrium studies on the removal of $Cd^{2+}$ ions from water using polyacrylamide grafted rice (Oryza sativa) husk and (Tectona grandis) saw dust, *J. Hazard. Mater.* **163,** 1338-44 **(2009)**

17. Elnasri N.A., Elsheik M.A., Eltayeb M.A., Physico-Chemical Characterization and Freundlich Isotherm studies of Adsorption of Fe(II), from aqueous solution by using Activated carbon prepared from Doum fruit waste, *Arch. Appl. Sci. Res.* **5,** 149-158 **(2013)**

18. Bhusari V.N., Dahake R., Rayalu S., Bansiwal A., Comparative study of removal of hexavalent chromium from water using metal oxide nanoparticles, *Adv. in Nanoparticles* **5,** 67-74 **(2016)**

19. Mustafa G., Tahir H., Sultan M., Akhtar N., Synthesis and characterization of cupric oxide (CuO) nanoparticles and their application for the removal of dyes, *Afr. J. Biotechnol*. **12,** 6650-6660 **(2013)**

20. Sharma N., Singh J., Sharma A., Removal of $Zn^{+2}$ ions from aqueous solution using rice (*oryza sativa*) husk in a sequential bed adsorption column, *Int. J. Environ. Technol. Manage*. **12,** 333-343 **(2010)**

21. Saraf S., Vaidya V.K., Elucidation of Sorption Mechanism of R. arrhizus for Reactive Blue 222 using Equilibrium and Kinetic Studies, *J. Microb. Biochem. Technol*. **8,** 236-246 **(2016)**

22. Sotelo J.L., Ovejero G., Rodriguez A., Alvarez S., Garcia J., Adsorption of Carbamazepine in Fixed Bed Columns: Experimental and Modeling Studies, *Sep. Sci. Technol*. **48,** 2626-37 **(2013)**

23. A. P. Lim, A. Z. Aris, Continuous fixed-bed column study and adsorption modeling: Removal of cadmium (II) and lead (II) ions in aqueous solution by dead calcareous skeletons, *Biochem. Eng. J*. **87,** 50-61 **(2014)**

24. Rahman N., Khan M.F., Nitrate removal using poly-o-toluidine zirconium(IV)ethylenediamine as adsorbent: Batch and fixed-bed column adsorption modeling, *J. Water Process Eng.* **9,** 254-266 **(2016)**

**25.** Ayo M.D., Madufor I.C., , Onyeagoro G.A., Ogbobe O., Effect of filler characterization on the properties of chemically treated groundnut shell, *Macromolecules An Indian Journal* **11,** 043-050 **(2015)**

26. Bernal V., Erto A., Giraldo L., Moreno-Pirajan J.C., Effect of solution pH on the adsorption of paracetamol on chemically modified activated carbons, *Molecules* **22,**1032**(2017)** doi:10.3390/molecules22071032.